

Photooxidation of Self-Assembled Monolayers by Exposure to Light of Wavelength 254 nm: A Static SIMS Study

Nicholas J. Brewer,^{†,‡} Stefan Janusz,[§] Kevin Critchley,^{||} Stephen D. Evans,^{||} and Graham J. Leggett^{*,§}

Department of Chemistry, UMIST, P.O. Box 88, Manchester M60 1QD, Department of Chemistry, University of Sheffield, Brook Hill, Sheffield S3 7HF, and School of Physics and Astronomy, University of Leeds, Leeds LS2 9JT, United Kingdom

Received: December 13, 2004; In Final Form: April 11, 2005

Self-assembled monolayers (SAMs) of alkanethiols have been photooxidized by exposure to light from a lamp emitting light with a wavelength of 254 nm. The data confirm that SAM oxidation on exposure to UV light sources occurs in the absence of ozone, but also suggest that the mechanism is different from that observed in previous studies using broad-spectrum arc lamps. In particular, for monolayers on both gold and silver, carboxylic acid-terminated SAMs oxidize significantly faster than methyl-terminated SAMs, in contrast to earlier observations for monolayers exposed to light from a mercury arc lamp. The difference in rates of photooxidation for the two classes of monolayer is significantly greater on silver than on gold. These data support our recent suggestion that while methyl-terminated SAMs are able to pack much more closely on silver than on gold, carboxylic acid-terminated thiols are not able to adopt the same close-packed structures, and their rates of photooxidation on silver are similar to, or slightly greater than, those measured for the same adsorbates on gold. Surface potential measurements were made for carboxylic acid- and methyl-terminated SAMs using a Kelvin probe apparatus. It was found that the work functions of carboxylic acid-terminated SAMs are significantly greater than those of methyl-terminated monolayers. It is concluded that these data are consistent with the oxidation reaction being initiated by “hot” electrons generated following the interaction of photons with the metallic substrate.

Introduction

Self-assembled monolayers (SAMs) have attracted widespread interest for both fundamental investigations of interfacial phenomena (including biological interactions with surfaces,^{1–8} adhesion,^{9–12} wetting,^{13–16} and friction and lubrication^{17–24}) and as templates for the fabrication of complex molecular architectures from macroscopic to nanometer dimensions.^{25–33} A variety of methods have been reported for the patterning of SAMs. Perhaps the most widely used is micro contact printing.²⁷ However, photopatterning has been established for a decade now and provides a convenient route to chemically well-defined, contamination-free patterns with low defect densities.^{34–41} Recent research in the authors’ laboratory has established that a new approach to SAM photopatterning, which we term scanning near-field photolithography (SNP), in which a scanning near-field optical microscope coupled to a UV laser is employed as the light source, may facilitate the routine fabrication of structures of size 30–40 nm^{42,43} and frequently much smaller.⁴⁴ The smallest feature size achieved to date (a line width of 13 nm, corresponding to $\lambda/20$) rivals the performance of electron beam lithography. SNP has proved to be a flexible and versatile tool, facilitating the fabrication of metallic nanotrenches using nanopatterned SAMs as resists, and the attachment of proteins

and nanoparticles to yield organic and biological nanostructures. To properly explore the possibilities offered by SNP for patterning on the nanometer scale, it is necessary to have a better understanding of the mechanism and kinetics of SAM photooxidation at appropriate wavelengths. Previously published studies of SAM photochemistry have utilized broad-spectrum UV sources such as arc lamps.^{34–40,45–49} There have been few attempts to investigate photochemistry using single-wavelength sources. This lack of fundamental data led some authors to speculate that SAM oxidation on exposure to UV light sources was not, in fact, a photochemical process, but was caused by ozone generated by short-wavelength UV light.^{50–53} Recently we demonstrated that this was not the case,⁵⁴ by using an ozone-free source, emitting principally at 254 nm, to photochemically oxidize SAMs. This finding was particularly important in the context of our efforts to develop near-field photolithographic methods for SAM patterning, because it is unlikely that a method based upon the formation of gaseous ozone would provide a readily controlled route to the fabrication of nanometer-scale patterns.

To fully characterize the conditions required to photopattern SAMs, we have compared the rates of photooxidation of a variety of adsorbates, with both methyl and carboxylic acid terminal groups, adsorbed on both gold and silver surfaces. Our objective was to determine the dependence of the rate of photooxidation on the adsorbate terminal group, alkyl chain length, and sulfur–metal chemistry. The work of Grunze and co-workers, for example, has provided a large body of evidence that these factors influence the degradation of SAMs exposed to electrons and to plasmas.^{55–60} In earlier studies it was also

* To whom correspondence should be addressed. E-mail: Graham.Leggett@shef.ac.uk.

[†] UMIST.

[‡] Present address: Faculty of Life Sciences, Dundee University, Nethergate, Dundee DD1 4HN, U.K.

[§] University of Sheffield.

^{||} University of Leeds.

shown that the nature of the adsorbate tail group had a strong influence on the kinetics of oxidation on exposure of SAMs to light from a mercury arc lamp,^{49,54} and evidence was provided that the mechanisms of oxidation on gold and silver were different.^{46,48} Here we examine whether similar correlations may be made for SAMs exposed to light of wavelength 254 nm. Such an improved mechanistic understanding of SAM photochemistry is important not only for SAM nanophotopatterning, but also for understanding the factors that determine the stability of SAMs under exposure to ambient oxygen.^{61–63} There has been a great deal of speculation about whether the ambient oxidation of SAMs occurs via an ozonolysis mechanism or by the photochemical oxidation of adsorbates, for example.

Experimental Section

Self-assembled monolayers were prepared by immersing freshly prepared Cr-primed, gold-coated glass microscope slides in 1 mmol dm⁻³ solutions of alkanethiols in degassed ethanol for 18 h. Cr was deposited onto glass microscope slides (no. 2 thickness, Chance Proper Ltd., U.K.) to a thickness of 2 nm, and gold was deposited to a thickness of 25 nm, at a rate of 0.1 nm s⁻¹. All glassware was cleaned prior to use by immersion in piranha solution (3 parts hydrogen peroxide to 7 parts concentrated sulfuric acid) for 30 min, followed by rinsing in copious quantities of deionized water and drying in an oven. *Caution: Piranha solution may detonate unexpectedly on contact with organic material!* Dodecanethiol (abbreviated C₁₁-CH₃ hereafter), butanethiol (BT, C₃CH₃), and mercaptopropanoic acid (C₂COOH) were obtained from Fluka at a purity of 97% and used as received. Mercaptoundecanoic acid (MUA, C₁₀COOH) was obtained from Aldrich and recrystallized twice from hexane prior to use. Advancing water contact angles were measured for representative SAMs and compared with literature values, to ensure monolayer purity was maintained.

Secondary ion mass spectrometry was carried out on a Vacuum Generators system equipped with a VG MM 12-12 quadrupole mass analyzer and a VG gallium liquid metal ion gun. The gun was run at an emission potential of 10 keV in both positive and negative ion mode. The beam was rastered over a 5 × 5 mm area with a current of less than 5 × 10⁻⁹ A cm⁻², and the analysis time was adjusted so that a dose of 5 × 10¹² ions cm⁻² was not exceeded, thus remaining well within the static limit usually set at 10¹³ ions cm⁻².

Ultraviolet (UV) exposure was from an ozone-free UV Lamp (model R-52G, UVP Inc., Cambridge, U.K.). The majority of emission from this lamp occurs at 254 nm, with a power of 1.25 mW cm⁻² at a distance of 15 cm. To confirm the manufacturer's claim that the lamp was ozone-free, we tested for ozone using a Draeger tube (Draeger Safety, Northumbria, U.K.). Ozone was undetectable at the lower limit of sensitivity of 0.005 ppm. The lamp achieves ozone-free emission by utilizing a filter designed to eliminate light with the shorter wavelengths (<200 nm) known to initiate ozone formation.

Surface potentials were determined using a home-built Kelvin probe apparatus. An *x*, *y*, *z* stage was used to move samples under a platinum probe (area 2.7 mm²). The probe was vibrated at a frequency of 800 Hz using a piezoactuator (P200-16, Linos Photonics), to create an alternating current. The contact potential difference (CPD) between the probe and the sample was determined using the null technique. The surface potential was calculated as the change in CPD between a substrate with a film and that of a freshly cleaned substrate.

Measurements were made six times on each of two samples from the same SAM, and these were repeated in triplicate from

SAMs made on different occasions. To remove the oxide layer from the silver, samples were immersed in a ferric nitrate solution before being immediately washed with purified water and then ethanol and dried under nitrogen before measurements were made.

Results

We have previously reported negative ion SIMS spectra of unoxidized monolayers of all of the adsorbates studied here, with the exception of C₂COOH. The spectra acquired in the present study reproduced the characteristic features of those data. For SAMs on gold, a peak is observed at *m/z* 197 that corresponds to Au⁻, together with a variety of highly characteristic molecular fragments, including Au(M - H)⁻ and Au-(M - H)₂⁻ (methyl-terminated thiols) and Au(M - CO₂H)⁻ (carboxylic acid-terminated thiols). Other ions were observed that correspond to gold-sulfur clusters and to fragments of the adsorbate molecules. The identities of these ions have been discussed at length elsewhere.^{48,49} Similarly, a range of molecular fragments were observed in the spectra of SAMs on silver that were consistent with previous studies and enabled verification that the fresh, as-prepared SAMs were free of evidence of oxidation. In particular, the intensity of the peak corresponding to AuMSO₃⁻ was negligible.

All of the SAMs studied were found to undergo oxidation on exposure to light with a wavelength of 254 nm. Oxidation was accompanied by changes in the SIMS spectra that were consistent with the behavior observed in earlier studies using a mercury arc lamp as the light source. After 10 min of exposure to UV light, a peak at *m/z* 265 was observed in the negative ion spectrum of C₁₀COOH on gold (Figure 1), corresponding to the sulfonate species MSO₃⁻. A peak was also observed at *m/z* 279 that is possibly due to (MSO₃ + C₂H₄)⁻. Prominent peaks were also observed at *m/z* 80 and 96 due to SO₃⁻ and SO₄⁻. After 20 and 45 min of exposure to UV light, the intensities of the peaks corresponding to AuS⁻ and AuS₂⁻ ions were observed to decrease significantly, and the intensity of the peak corresponding to Au(M - CO₂ - H)⁻ was observed to decrease. The peaks at *m/z* 80 and 96 increased significantly in intensity. The intensity of the peak due to the sulfonate species MSO₃⁻ increased as the length of exposure increased. A small peak was observed at *m/z* 221 for C₁₀COOH after exposure to UV light. It is possible that this peak indicates the elimination of CO₂ from the MSO₃⁻ species, yielding the stable anion CH₃(CH₂)₉SO₃⁻.

The behavior of C₁₁CH₃ was also found to be qualitatively similar to that observed in earlier studies using a mercury arc lamp, but importantly, the rate of change was much slower than observed for C₁₀COOH (Figure 2). After 10 min of exposure to UV light, prominent peaks were observed in the spectrum that are characteristic of unoxidized C₁₁CH₃, including AuS⁻ at *m/z* 229. Peaks that are characteristic of photooxidized C₁₁-CH₃, such as MSO₃⁻ at *m/z* 249 and (MSO₃ + CH₂)⁻, (MSO₃ + C₂H₄)⁻, and (MSO₃ + C₂H₄ + O)⁻ at *m/z* 263, 277, and 293 respectively, were also observed. Some of these species appear to result from photoinitiated reaction between adsorbate molecules. Peaks were observed at *m/z* 80 and 96 due to SO₃⁻ and SO₄⁻, but at this stage the peaks were relatively small. After 20 and 45 min of exposure to UV light, a peak may still be observed at *m/z* 229 that is due to AuS⁻, previously reported to correlate with the presence of intact adsorbate complexes. However, the sulfonate peaks were found to have increased in intensity, with (MSO₃)⁻, (MSO₃ + CH₂)⁻, (MSO₃ + C₂H₄)⁻, and (MSO₃ + C₂H₄ + O)⁻ becoming increasingly prominent. In addition, peaks due to SO₃⁻ and SO₄⁻ became very intense.

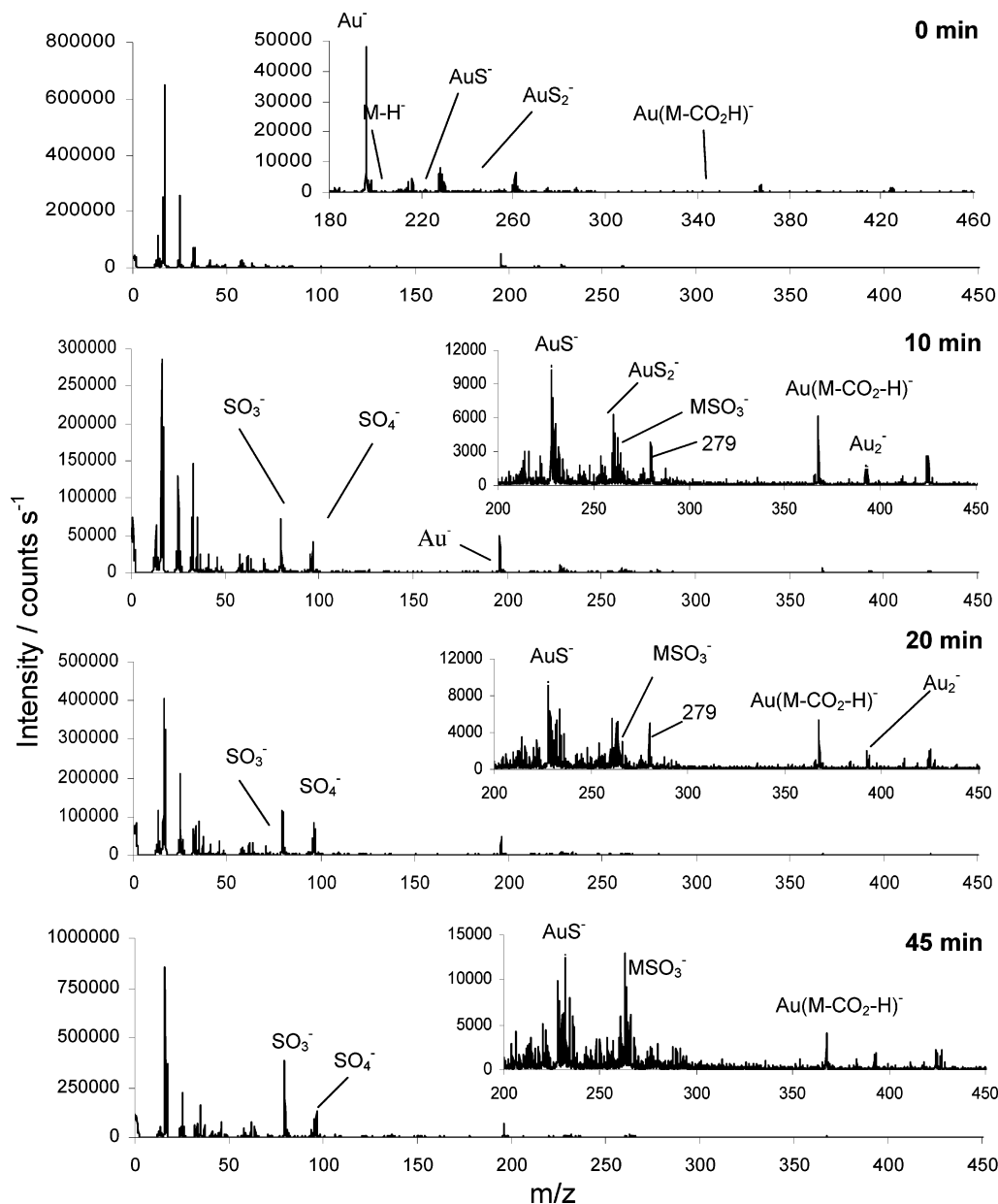


Figure 1. Static SIMS spectra of $C_{10}COOH$ on Au after increasing photooxidation times.

The behavior observed for C_2COOH on Au was similar to that observed for $C_{10}COOH$ (see Figure 3). After 10 min of exposure to UV light, some peaks that are characteristic of unoxidized C_2COOH were still evident, such as $Au(M-H)S^-$ and AuS^- at m/z 335 and 229, respectively. A peak was observed at m/z 258 which is due to $Au(M-CO_2-H)^-$. However, oxidation was evidenced by the appearance of a peak at m/z 153, due to the sulfonate species MSO_3^- , and at m/z 80 and 96, due to SO_3^- and SO_4^- . As exposure increased from 20 to 45 min, the sulfonate species increased in intensity so that by 45 min it was the dominant peak in the spectrum. The species that are characteristic of unoxidized SAMs decreased significantly in intensity.

After 10 min of exposure to UV light, the spectrum of C_3-CH_3 still exhibited prominent peaks due to unoxidized BT (for example, $Au(M-H)S^-$ and $Au(M-H)_2^-$ at m/z 318 and 375, respectively, and AuS^- and AuS_2^- at m/z 229 and 261, respectively; see Figure 4). There were some signs of photooxidation with a small MSO_3^- peak appearing at m/z 137 and

a SO_3^- peak at m/z 80. After 20 and 45 min of exposure to 254 nm UV light, the peaks characteristic of unoxidized BT declined in intensity; however, even after 45 min of exposure, molecular fragments containing unoxidized adsorbates were still observed with significant intensity. By 45 min the sulfonate peak was the most intense in the spectrum, indicating that significant oxidation had occurred.

When monolayers of $C_{10}COOH$ on silver were exposed to UV light, there were significant changes (Figure 5). After 10 min of exposure, there were still peaks that correspond to unoxidized MUA such as $Ag(M-H)^-$ at m/z 324/26 and AgS^- at m/z 139/141. However, the $(M-H)^-$ peak was significantly reduced in intensity compared to that in the spectrum of the unoxidized adsorbate, and a peak was observed at m/z 265, corresponding to the sulfonate, together with a peak at m/z 80, indicative of SO_3^- . A peak was also observed at m/z 279/281, probably corresponding to $Ag(M-CO_2-H)^-$. After 20 min of exposure to UV light, the sulfonate peak and the SO_3^- peak

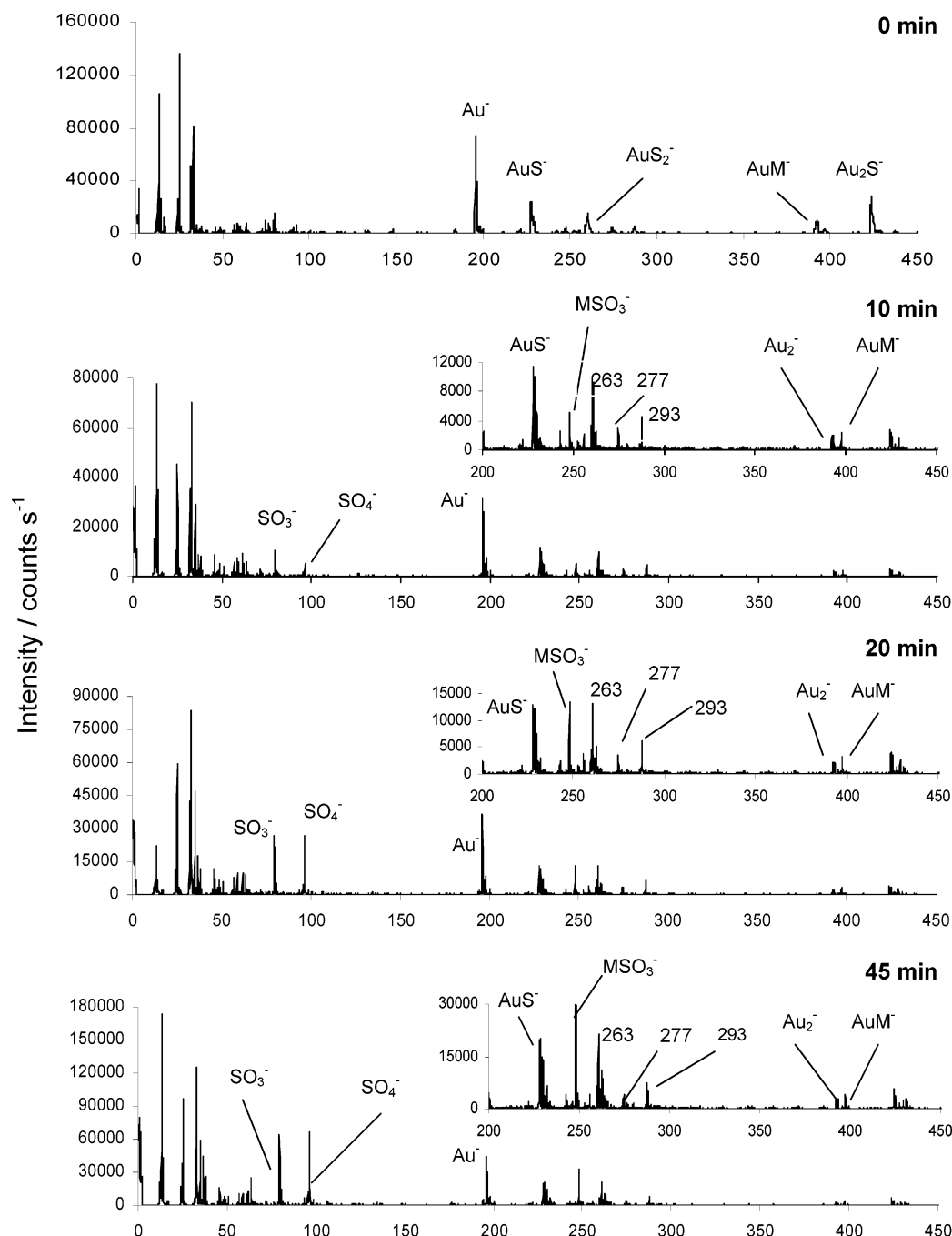


Figure 2. Static SIMS spectra of $C_{11}CH_3$ on Au after increasing photooxidation times.

increased in intensity, and an intense SO_4^- peak was observed at m/z 96. Peaks that corresponded to the unoxidized MUA were weaker. The $M - H^-$ peak at m/z 217 was of negligible intensity, and the $Ag(M - H)^-$ and AgS^- peaks were also weak. After 60 min of exposure to UV light the peaks corresponding to oxidation products dominated the spectrum. Some AgS^- was still observed at m/z 139/141, but the peak was very weak.

Photooxidation in the other SAMs on silver followed qualitatively similar trends (the spectra are shown in the Supporting Information for this paper). Quantitatively, however, there were significant differences between the behaviors of carboxylic acid- and methyl-terminated SAMs, as was observed for monolayers on gold. $C_{11}CH_3$ exhibited a small sulfonate peak after 60 min of exposure, and only slightly diminished silver molecular fragments; this behavior was also observed for C_3CH_3 , although the sulfonate peak was stronger after 60 min

than was the case for $C_{11}CH_3$. C_2COOH oxidized rapidly, exhibiting a rapid decline in the intensities of the silver molecular peaks and a concomitant growth in the sulfonate peak.

A quantitative analysis of the SIMS data was conducted. While the quantification of absolute SIMS ion intensity data has been the subject of some controversy, it has been established that, using the method of relative intensity measurement of Vickerman and co-workers,^{64,65} it is possible to quantify changes in surface composition and bonding. Such approaches have been successfully applied to organic systems, including, for example, block copolymers.⁶⁶ In earlier studies we demonstrated that for SAMs exposed to a mercury arc lamp, SIMS data could be analyzed using Vickerman's approach and were found to be a valuable measure of SAM photooxidation.^{40,48,49,54} For example, for $C_{11}CH_3$, the time required for complete oxidation was determined using this approach⁴⁹ and by using XPS⁴⁷ to be

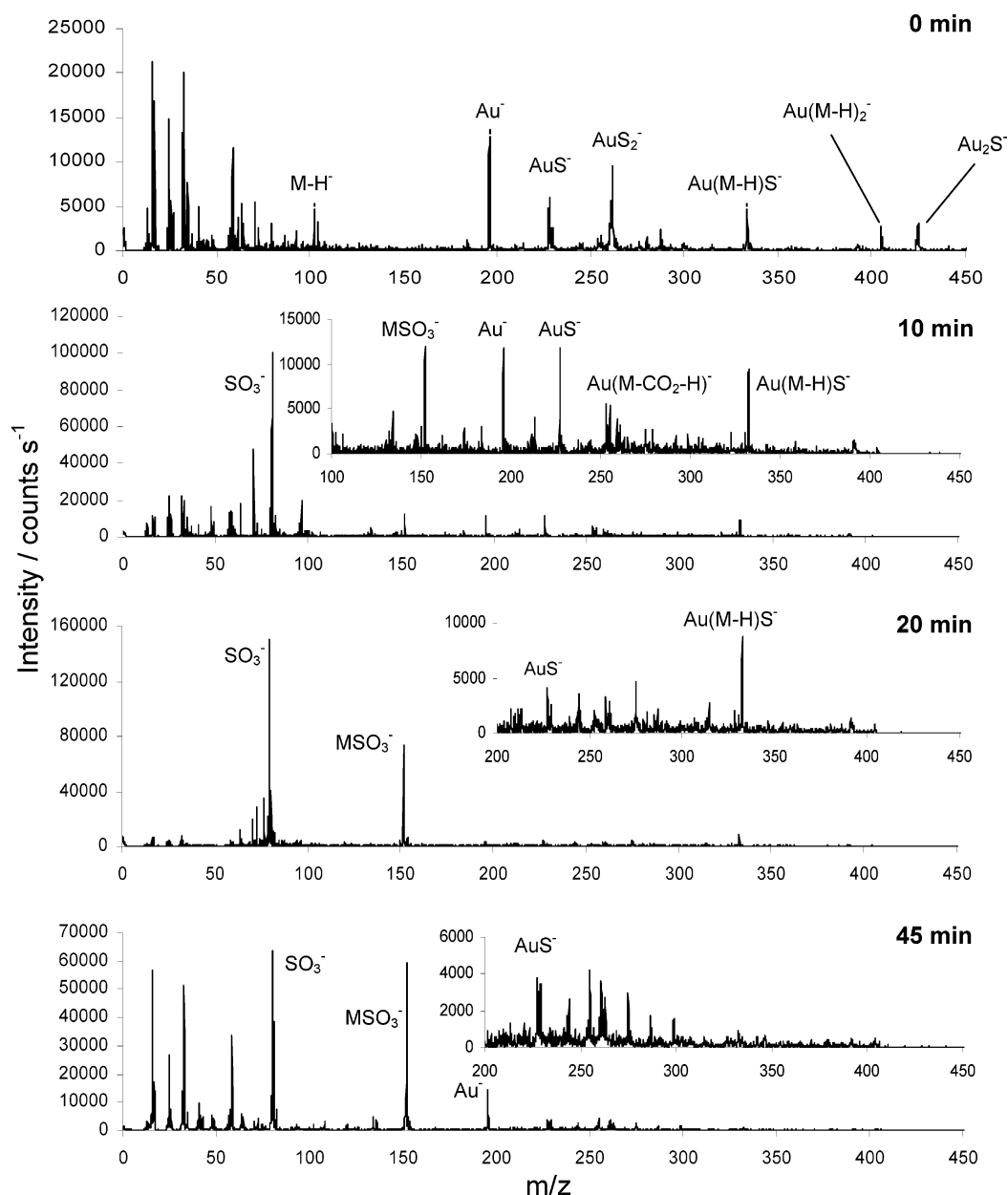
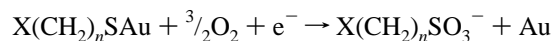


Figure 3. Static SIMS spectra of C_2COOH on Au after increasing photooxidation times.

approximately 2 h using a mercury arc lamp source. Here we have used the same approach as described in our earlier work. The photooxidation reaction is thought to occur according to the equation



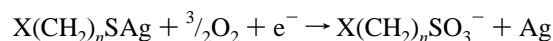
For the short-chain adsorbates, the extent of oxidation χ_t at time t is determined from the ratio of the sulfonate peak intensity, $[MSO_3^-]$, to that of the dominant gold molecular fragment, $[Au(M-H)S^-]$:

$$\chi_t = [MSO_3^-] / ([MSO_3^-] + [Au(M-H)S^-])$$

For the long-chain adsorbates, the corresponding molecular fragments are weaker and data are subject to more noise. Instead, the intensity of the AuS^- peak may be used:^{48,49}

$$\chi_t = [MSO_3^-] / ([MSO_3^-] + [AuS^-])$$

For SAMs on silver, the equation for the photooxidation reaction is similar:



The extent of reaction may be determined in a similar way from the intensities of the respective molecular fragments:

$$\chi_t = [MSO_3^-] / ([MSO_3^-] + [M-H]^-)$$

In this case it should be noted that the use of molecular fragments is essential throughout because a competing reaction, involving scission of the S–C bond, occurs.^{46,48} We demonstrated earlier that while XPS fails to differentiate between the two pathways, SIMS enables them to be distinguished and by tracking only the molecular species (as opposed to the elemental species) it is possible to look specifically at the rate of conversion of alkanethiolates to alkylsulfonates.⁴⁸ Yields of molecular fragments were substantially greater on silver than

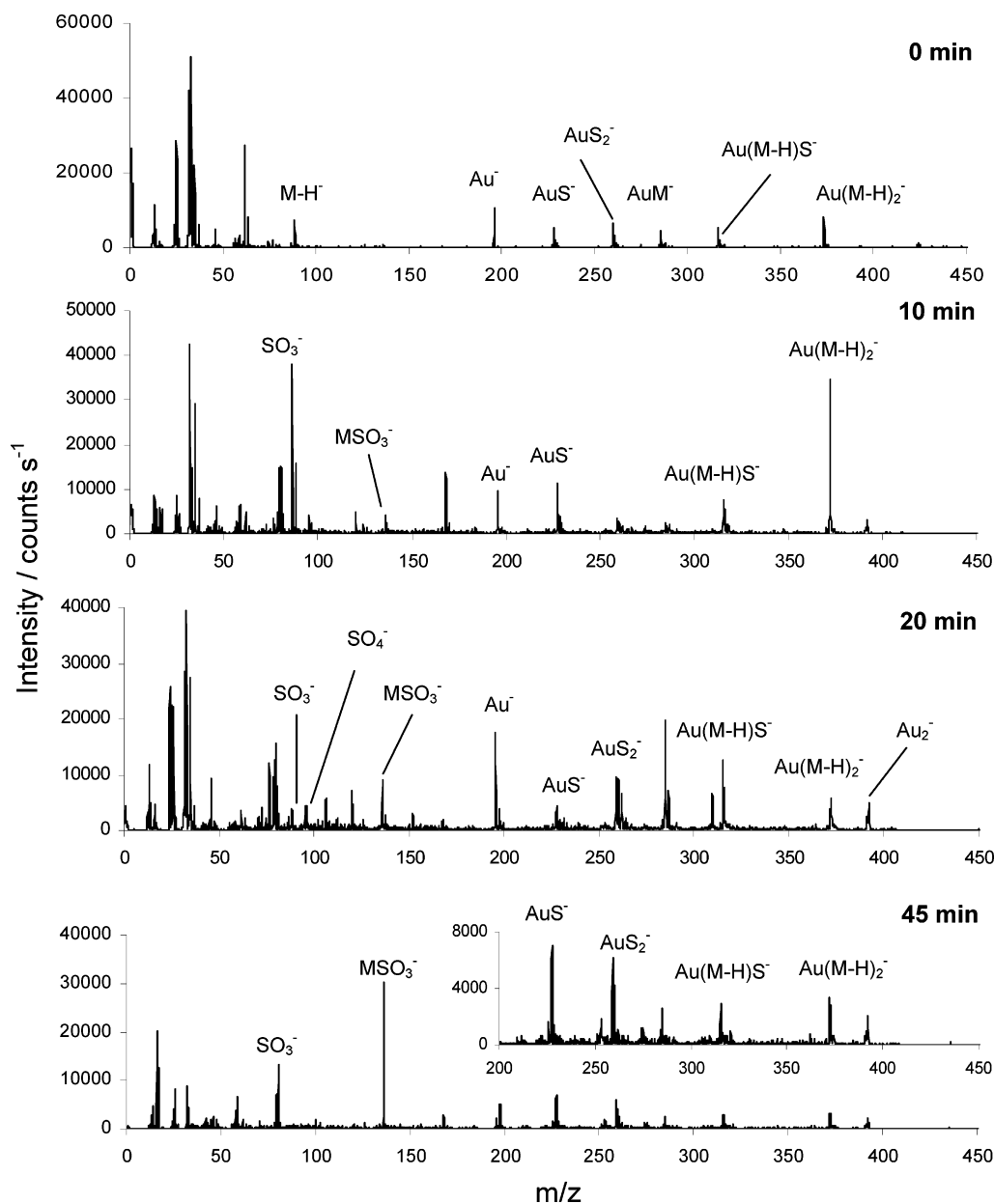


Figure 4. Static SIMS spectra of C_3CH_3 on Au after increasing oxidation times.

on gold, so that, even for the long-chain adsorbates, it was possible to use the intensities of metal molecular fragments to calculate the extent of oxidation.

The resulting data on the extent of photooxidation are shown in Figure 6. Because of the intrinsic variability of spectra, the data shown in Figure 6 are the means of, typically, three measurements. On gold, in agreement with the qualitative data, it may be seen that C_2COOH oxidizes the fastest, with complete oxidation occurring after around 20 min. The emission of our lamp is ca. 1 mW cm^{-2} at 254 nm, so this corresponds to a dose of ca. 1.2 J cm^{-2} . The next fastest is C_3CH_3 , with $C_{10}COOH$ close behind. The slowest rate of oxidation was observed for $C_{11}CH_3$, which after an exposure of 60 min (ca. 3.6 J cm^{-2}) is extensively, but not completely, photooxidized. On silver, the trends are similar—short-chain adsorbates oxidize faster than long-chain adsorbates with the same terminal group—but the difference between the rates of oxidation of methyl- and carboxylic acid-terminated adsorbates with the same chain length is greater.

A simple kinetic analysis was carried out, assuming first-order kinetics and plotting $\ln \chi_i$ vs t to yield a straight line with

a gradient equal to the pseudo rate constant for the reaction, k_{Au} on gold and k_{Ag} on silver (Figure 7). Although not a rigorous mechanistic analysis, this approach yields a numerical parameter that may be used to compare reactions. The data are shown in Table 1. The data support the qualitative conclusions drawn from Figure 5. For each chain length and for both substrates, the carboxylic acid-terminated adsorbates oxidize faster than the methyl-terminated adsorbates. For each terminal group, the short-chain adsorbates oxidize faster than the long-chain adsorbates. For methyl-terminated adsorbates, the SAMs oxidize faster on gold than is the case for the same adsorbates on silver. In contrast, however, for the carboxylic acid-terminated adsorbates, rates of photooxidation on silver are similar to, or larger than, rates of photooxidation of the same adsorbates on gold.

The surface potentials of SAMs on Ag and Au were measured using the Kelvin probe apparatus. The resulting work function data are shown in Table 2. The work functions of the polar SAMs are larger than those of the methyl-terminated monolayers for both metals. In general the work functions of the long-chain adsorbates are larger than those of their shorter analogues, although the difference is small. The exception to this is the

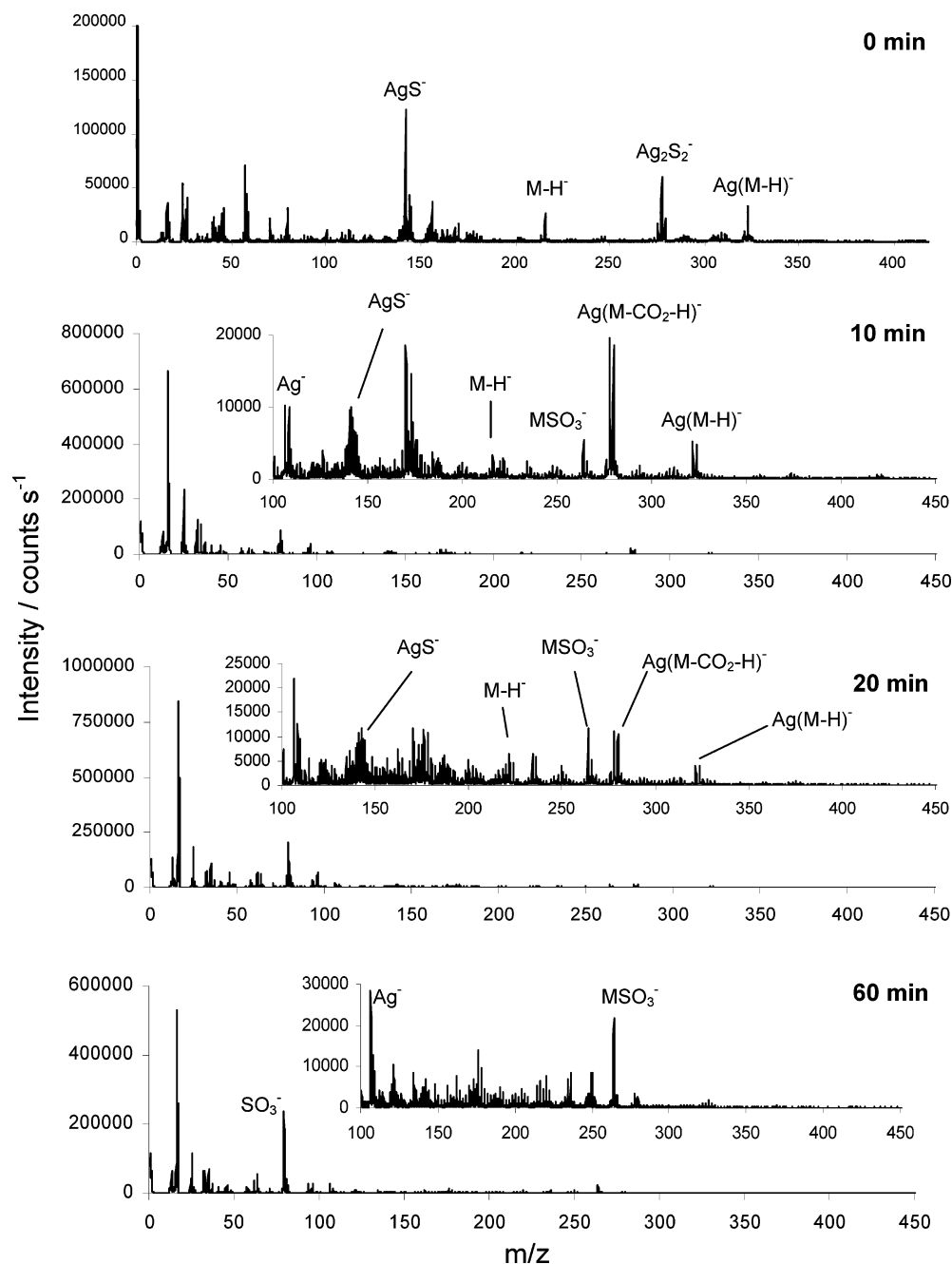


Figure 5. Static SIMS spectra of $C_{10}COOH$ on Ag after increasing photooxidation times.

case of the carboxylic acid-terminated adsorbates on silver, although the discrepancy here lies within the bounds of experimental error ($\pm 5\%$).

Discussion

These detailed investigations support our earlier conclusion that photochemical oxidation of alkanethiol SAMs occurs on exposure to UV light with a wavelength of 254 nm.⁵⁴ The lamp used in this study was fitted with a filter designed to eliminate the short-wavelength light that initiates ozone formation, so the mechanism clearly does not involve ozonolysis. On the basis of the data presented here, we are able to make further conclusions concerning the mechanism of photooxidation.

Adsorbate Packing Has a Strong Influence on the Rate of Photooxidation. In an earlier study of SAM photooxidation,⁴⁷ we showed that, for methyl-terminated SAMs exposed to light from a mercury arc lamp, the rate constant for the photooxi-

dation reaction increased with decreasing adsorbate chain length. It was concluded that the rate-determining step in the photooxidation reaction was penetration of oxygen species to the Au–S bond. The present data are in agreement with this. On gold, the rate constant for the photooxidation reaction for C_3-CH_3 is approximately twice that for $C_{11}CH_3$. The difference is even larger on Ag. Short-chain adsorbates pack less closely than alkanethiols with longer alkyl chains, so that penetration of oxygen between the adsorbate molecules is easier.

For methyl-terminated SAMs in the present study, k_{Ag} was significantly smaller than k_{Au} , suggesting more rapid penetration of oxygen to the metal–sulfur bond on gold than on silver. This is consistent with the substantive body of literature reporting closer packing of methyl-terminated thiols on silver than on gold.^{67–69} For example, the tilt angle of alkanethiols on silver is somewhat smaller at 12° than the values of ca. 30° typically reported on gold.⁶⁷ The spacing between adsorption sites in the

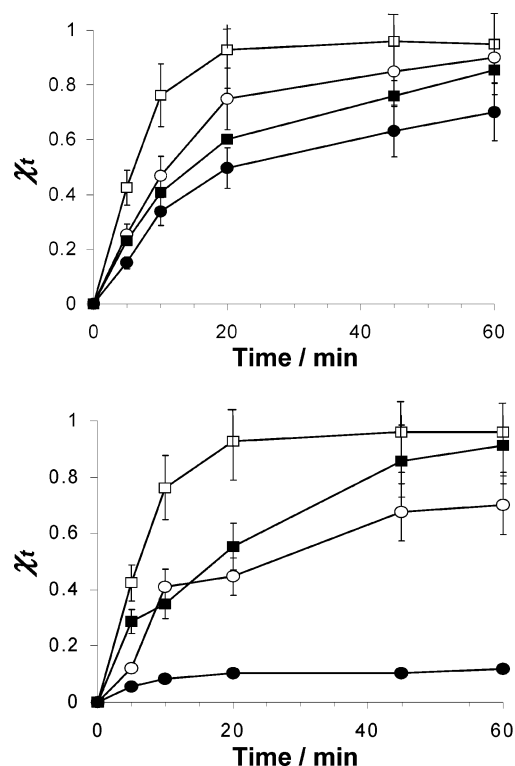


Figure 6. Variation of the extent of oxidation χ_t of SAMs with time of exposure to UV light: top, gold substrates; bottom, silver substrates. Key: \circ , C_3H_3 ; \bullet , $C_{11}CH_3$; \square , C_2COOH ; \blacksquare , $C_{10}COOH$.

TABLE 1: Kinetic Data for SAM Photooxidation

adsorbate	k_{Au}/min^{-1}	k_{Ag}/min^{-1}	adsorbate	k_{Au}/min^{-1}	k_{Ag}/min^{-1}
C_2COOH	0.1339	0.1339	C_3CH_3	0.0371	0.0198
$C_{10}COOH$	0.0325	0.0405	$C_{11}CH_3$	0.0200	0.0015

TABLE 2: Work Function Data for SAMs

adsorbate	Φ_{Au}/eV	Φ_{Ag}/eV	adsorbate	Φ_{Au}/eV	Φ_{Ag}/eV
C_2COOH	5.64	5.09	C_3CH_3	4.98	4.58
$C_{10}COOH$	5.53	5.22	$C_{11}CH_3$	4.78	4.36

$(\sqrt{3} \times \sqrt{3})R30$ arrangement adopted by methyl-terminated SAMs on gold is ca. 5 Å, compared to 4.4 Å on silver. On silver the diffusion of oxygen species to the sulfur–metal bond would thus be expected to be impeded.

For carboxylic acid-terminated SAMs, the rate constant for the photooxidation reaction was larger for the short-chain SAMs than for the long-chain adsorbates, again consistent with expectations that the reduced order in the short-chain systems

will render the passage of oxygen to the metal–sulfur bond more rapid. However, in contrast to the methyl-terminated SAMs, which exhibited significantly smaller rate constants on silver, the carboxylic acid-terminated SAMs exhibited k_{Ag} values that were similar to, or slightly larger than, the k_{Au} values measured for the same adsorbates. This suggests that, for these adsorbates, penetration of oxygen to the sulfur–metal bond is easier (or, at least, no more difficult) on silver than on gold, implying that carboxylic acid-terminated molecules pack differently from the methyl-terminated thiols. This conclusion is consistent with recent work in the authors' laboratory using friction force microscopy (FFM) to probe the organization of SAMs on silver and gold. It was demonstrated that the friction coefficients of methyl-terminated SAMs on silver were approximately half the values measured for monolayers of the same adsorbates on gold, reflecting the closer packing and the greater difficulty of inducing gauche defects and other conformational changes as the tip slides across the sample, while carboxylic acid-terminated thiols exhibited coefficients of friction on silver that were similar to, or larger than, those measured for the same adsorbates on gold. Comparatively little is known about the structures of monolayers of alkanethiols with polar terminal groups adsorbed on silver. However, on the basis of our FFM data, we suggested that the bulk of the carboxylic acid group meant that the acid-terminated adsorbates were unable to adopt the highly close-packed structure adopted by methyl-terminated adsorbates on silver, adopting a different structure commensurate with the dimensions of the adsorbate. The rate constants reported here are clearly consistent with this hypothesis. The present data thus provide corroboration for our earlier predictions and underline the value of FFM data in fundamental investigations of molecular organization at surfaces.

Photooxidation Is Initiated by the Formation of “Hot” Electrons at the Gold Surface. It has remained unclear what the causative agent is in the photooxidation of alkanethiol SAMs. While exposure to ozone does cause oxidation, it is clear that this is not necessary for SAM oxidation. In their study, Huang and Hemminger speculated that hot electrons, formed by the absorption of photons by electrons in the substrate, were the most likely causative agent.³⁶ However, this early hypothesis has been largely ignored. We believe that, in conjunction with the measurements reported here of SAM surface potentials, the present data on photooxidation kinetics are consistent with oxidation stimulated by hot electron formation. While one must make the caution that surface potentials measured using a Kelvin probe are based upon an analysis of the entire SAM system, and hot electrons are likely to be injected into a state very close

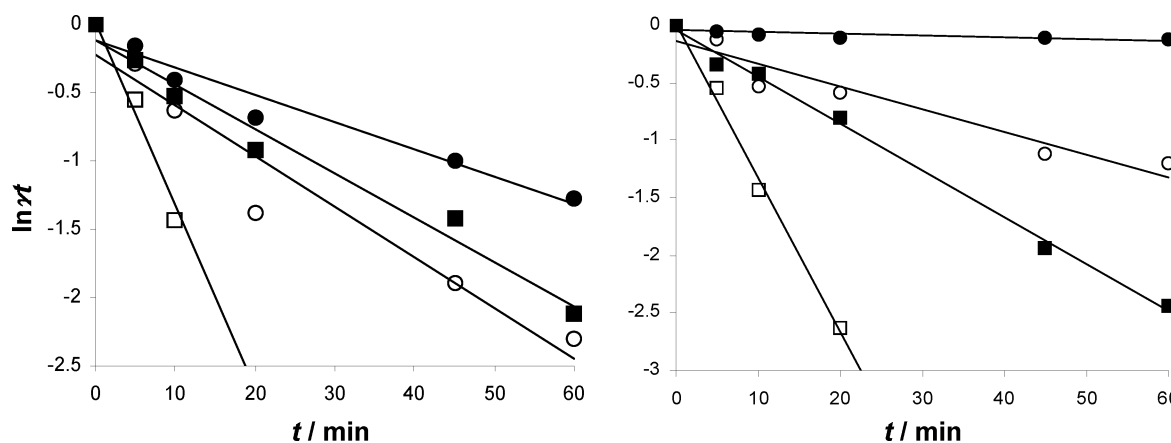


Figure 7. Variation in $\ln \chi_t$ with t for monolayers on gold (left) and silver (right). Key: \circ , C_3H_3 ; \bullet , $C_{11}CH_3$; \square , C_2COOH ; \blacksquare , $C_{10}COOH$.

to the metal surface, where the local potential may be different, the data in Table 2 provide a useful indication of the likely impact of adsorbate molecular structure on the behavior of hot electrons at the Au surface. Surface potentials of SAMs vary with the length of the alkyl chain⁷⁰ and with the nature of the terminal group functionality,⁷¹ because both may alter the net dipole moment of the adsorbate. For methyl-terminated thiols, the dipole moment increases with the alkyl chain length, with the result that the air–monolayer interface becomes progressively positive with respect to the gold–sulfur interface. This increases the magnitude of the surface potential, and effectively reduces the barrier to electron emission (i.e., it effectively reduces the work function). In contrast, the adsorption of molecules with electronegative terminal groups (as in the case of carboxylic acid-terminated thiols in the present study) creates a surface dipole with opposite orientation; the result is a net increase in the energy barrier to electron emission (i.e., it increases the work function).

The large difference in the rates of photooxidation of SAMs with the same chain length and different tail groups observed here is particularly important. For adsorbates of a given length, carboxylic acid-terminated monolayers oxidize faster than methyl-terminated ones on both metals. The magnitude of the difference is greatest on silver. The behavior observed here is the reverse of the behavior observed when SAMs are exposed to light from an arc lamp, when methyl-terminated SAMs have been shown to oxidize the fastest.⁴⁹ In an earlier study the enhanced stability of acid-terminated SAMs exposed to an arc lamp was attributed to the existence of hydrogen bonding between terminal groups,⁴⁹ which confers an additional stabilization on the monolayers (estimated to be as much as 33 kJ mol⁻¹).⁴⁰ Clearly there is a difference in the mechanism of oxidation on exposure to light from the 254 nm source used in the present study. The work function data suggest an explanation. Estimates of the work function of bare gold vary. However, on average, values (5.08 eV)⁷² are thought to be approximately similar to the photon energy (4.9 eV). Data acquired using the Kelvin probe apparatus suggest that the work functions of methyl-terminated SAMs are smaller than that of bare gold, while the work functions of carboxylic acid-terminated SAMs are larger. This means that, for methyl-terminated adsorbates, there is a possibility that absorption of a UV photon will lead to photoemission, albeit with very low kinetic energy and with a high probability that the electron will be strongly scattered by the adsorbate alkyl chains.⁷¹ The one exception to this is C₃H₇ on Au, which has a work function similar to the photon energy and, in any case, exhibits faster kinetics. However, for carboxylic acid-terminated SAMs, the photon energy is always less than the work function. Photoemission is unlikely. However, absorption of a photon may still lead to the formation of a hot electron⁷³ which, while it may not escape the surface, may tunnel into an excited state of an adsorbate sulfur atom (Figure 8).⁷⁴ This provides the trigger for the initiation of photooxidation. On silver the work function data support a similar explanation. The work functions are smaller than those of the corresponding thiols on gold, consistent with the fact that the work function of bare silver is typically smaller (ca. 4.73 eV⁷²) than that of gold. However, Φ was greater than the photon energy for both of the carboxylic acid-terminated SAMs, and smaller for both of the methyl-terminated adsorbates.

Arc Lamps Excite Other Oxidative Pathways. The different terminal group dependence of the oxidation reaction on exposure of SAMs to mercury arc lamps (carboxylic acid-terminated SAMs oxidize slower than methyl-terminated ones) suggests

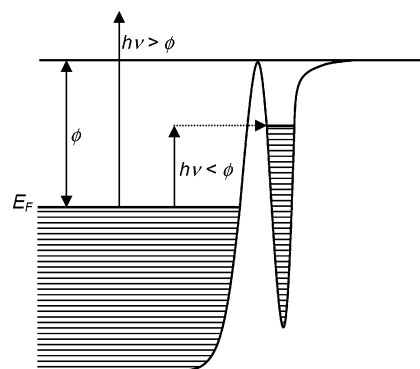


Figure 8. Schematic diagram illustrating two processes that may occur on exposure of a SAM to UV light. When the incident photon energy is greater than the work function, electron emission may occur. When the incident photon energy is less than the work function, creation of hot electrons may occur. These may tunnel through into the potential well of an adsorbate sulfur atom; inelastic transfer of the electron to the gold surface may leave the adsorbate in an excited state, initiating oxidation.

either that the mechanism of oxidation is different or that additional processes occur. We speculated that the existence of hydrogen bonds between adsorbate terminal groups leads to stabilization of carboxylic acid-terminated SAMs. This is consistent with the suggestion⁴⁷ that penetration of active oxygen species is the rate-limiting step in SAM photooxidation. In the case of the arc lamp, it seems that active species formed in the gas phase diffuse through the monolayer and react with adsorbate headgroups. At 254 nm, the rate of oxygen diffusion is clearly a significant parameter but the rate of hot electron attachment to adsorbate sulfur atoms is also critical. In the case of arc lamp exposure, it is possible that ozonolysis^{50–53} and/or the formation of singlet oxygen species⁴⁷ are significant contributors. While emission does occur at 254 nm from mercury arc lamps, their spectra are complex, and many other, stronger lines are observed. These tail off at short wavelengths, but there may also be adequate short-wavelength emission for the generation of ozone and other species. The exact mechanism clearly requires clarification.

Conclusions

Exposure of self-assembled monolayers of alkanethiols on gold and silver to 254 nm light leads to photochemical oxidation. For both methyl- and carboxylic acid-terminated adsorbates, oxidation is faster for short-chain adsorbates than for long-chain ones. On silver, methyl-terminated adsorbates oxidize significantly slower than they do on gold, consistent with the expected increase in the packing density of adsorbates, slowing the diffusion of oxygen to the metal–sulfur bond. For carboxylic acid-terminated adsorbates, rate constants for the photooxidation reaction on silver are similar to or slightly larger than those measured on gold, consistent with a recent friction force microscopy study which suggested that carboxylic acid-terminated thiols are not able to pack as closely on silver as methyl-terminated ones, and instead adopt a more open structure able to accommodate the bulkier terminal group. The data presented here are consistent with the hypothesis that photooxidation on exposure to 254 nm light occurs through a mechanism initiated by hot electron formation at the surface of the metal substrate, and is different from the mechanism that operates on exposure of SAMs to mercury arc lamps.

Acknowledgment. N.J.B. and S.J. thank the EPSRC for research studentships. G.J.L. thanks the EPSRC and the RSC Analytical Chemistry Trust Fund for financial support.

Supporting Information Available: Static SIMS spectra of unoxidized SAMs and static SIMS spectra of oxidized SAMs on silver. This material is available free of charge via the Internet at <http://pubs.acs.org>.

References and Notes

- (1) Lopez, G. P.; Albers, M. W.; Schrieber, S. L.; Carroll, R.; Peralta, E.; Whitesides, G. M. *J. Am. Chem. Soc.* **1993**, *115*, 5877.
- (2) Singhvi, R.; Kumar, A.; Lopez, G. P.; Stephanopoulos, G. N.; Wang, D. I. C.; Whitesides, G. M.; Ingber, D. E. *Science* **1994**, *264*, 696.
- (3) Mrksich, M.; Whitesides, G. M. *Annu. Rev. Biophys. Biomol. Struct.* **1996**, *25*, 55.
- (4) Brock, A.; Chang, E.; Ho, C.-C.; LeDuc, P.; Jiang, X.; Whitesides, G. M.; Ingber, D. E. *Langmuir* **2003**, *19*, 1611.
- (5) Tidwell, C. D.; Ertel, S. I.; Ratner, B. D.; Tarasevich, B. J.; Atre, S.; Allara, D. L. *Langmuir* **1997**, *13*, 3404.
- (6) McClary, K. B.; Grainger, D. W. *Biomaterials* **1999**, *20*, 2435.
- (7) Cooper, E.; Parker, L.; Scotchford, C. A.; Downes, S.; Leggett, G. J.; Parker, T. L. *J. Mater. Chem.* **2000**, *10*, 133.
- (8) Keselowsky, B. G.; Collard, D. M.; Garcia, A. J. *J. Biomed. Mater. Res., A* **2003**, *66*, 247.
- (9) Frisbie, C. D.; Rozsnyai, L. F.; Noy, A.; Wrighton, M. S.; Lieber, C. M. *Science* **1994**, *265*, 2071.
- (10) Noy, A.; Frisbie, C. D.; Rozsnyai, L. F.; Wrighton, M. S.; Lieber, C. M. *J. Am. Chem. Soc.* **1995**, *117*, 7943.
- (11) Fisher, G. L.; Hooper, A. E.; Opila, R. L.; Allara, D. L.; Winograd, N. *J. Phys. Chem. B* **2000**, *104*, 3267.
- (12) Hooper, A.; Fisher, G. L.; Konstadinidis, K.; Jung, D.; Nguyen, H.; Opila, R.; Collins, R. W.; Winograd, N.; Allara, D. L. *J. Am. Chem. Soc.* **1999**, *121*, 8052.
- (13) Bain, C. D.; Whitesides, G. M. *Science* **1988**, *240*, 62.
- (14) Bain, C. D.; Biebuyck, H. A.; Whitesides, G. M. *Langmuir* **1989**, *5*, 723.
- (15) Nuzzo, R. G.; Dubois, L. H.; Allara, D. L. *J. Am. Chem. Soc.* **1990**, *112*, 558.
- (16) DuBois, L. H.; Zegarski, B.; Nuzzo, R. G. *J. Am. Chem. Soc.* **1990**, *112*, 570.
- (17) Green, J.-B.; McDermott, M. T.; Porter, M. D.; Siperko, L. M. *J. Phys. Chem.* **1995**, *99*, 10960.
- (18) van der Vegte, E. W.; Hadziioannou, G. *Langmuir* **1997**, *13*, 4357.
- (19) Kim, H. I.; Graupe, M.; Oloba, O.; Koini, T.; Imaluddin, S.; Lee, T. R.; Perry, S. S. *Langmuir* **1999**, *15*, 3179.
- (20) Shon, Y. S.; Lee, S.; Colorado, S. S.; Perry, S. S.; Lee, T. R. *J. Am. Chem. Soc.* **2000**, *122*, 7556.
- (21) Brewer, N. J.; Beake, B. D.; Leggett, G. J. *Langmuir* **2001**, *17*, 1970.
- (22) Beake, B. D.; Leggett, G. J. *Phys. Chem. Chem. Phys.* **1999**, *1*, 3345.
- (23) Brewer, N. J.; Foster, T. T.; Leggett, G. J.; Alexander, M. R.; McAlpine, E. *J. Phys. Chem. B* **2004**, *108*, 4723.
- (24) Brewer, N. J.; Leggett, G. J. *Langmuir* **2004**, *20*, 4109.
- (25) Onclin, S.; Mulder, A.; Huskens, J.; Ravoo, B. J.; Reinhoudt, D. N. *Langmuir* **2004**, *20*, 5460.
- (26) Auletta, T.; Dordi, B.; Mulder, A.; Sartori, A.; Onclin, S.; Bruinink, C. M.; Peter, M.; Nijhui, C. A.; Beijleveld, H.; Schoenherr, H.; Vancso, J. G.; Casnati, A.; Ungaro, R.; Ravoo, B. J.; Huskens, J.; Reinhoudt, D. N. *Angew. Chem., Int. Ed.* **2004**, *43*, 369.
- (27) Xia, Y.; Whitesides, G. M. *Angew. Chem., Int. Ed.* **1998**, *37*, 551.
- (28) Piner, R. D.; Zhu, J.; Xu, F.; Mirkin, C. A. *Science* **1999**, *283*, 661.
- (29) Weinberger, D. A.; Hong, S.; Mirkin, C. A.; Wessels, B. W.; Higgins, T. B. *Adv. Mater.* **2000**, *12*, 1600.
- (30) Xu, S.; Liu, G.-Y. *Langmuir* **1997**, *13*, 127; Liu, G.-Y.; Amro, N. A. *Proc. Natl. Acad. Sci. U.S.A.* **2002**, *99*, 5165.
- (31) Zhou, D.; Wang, X.; Birch, L.; Rayment, T.; Abell, C. *Langmuir* **2003**, *9*, 10557.
- (32) Liu, M.; Amro, N. A.; Chow, C. S.; Liu, G.-Y. *Nano Lett.* **2002**, *2*, 863.
- (33) Zhou, D.; Sinniah, K.; Abell, C.; Rayment, T. *Angew. Chem., Int. Ed.* **2003**, *42*, 4934.
- (34) Tarlov, M. J.; Burgess, D. R. F.; Gillen, G. J. *Am. Chem. Soc.* **1993**, *115*, 5304.
- (35) Gillen, G.; Bennett, J.; Tarlov, M. J.; Burgess, D. R. F. *Anal. Chem.* **1994**, *66*, 2170.
- (36) Huang, J.; Dahlgren, D. A.; Hemminger, J. C. *Langmuir* **1994**, *10*, 626.
- (37) Wollman, E. W.; Kang, D.; Frisbie, C. D.; Lokovic, I. M.; Wrighton, M. S. *J. Am. Chem. Soc.* **1994**, *116*, 4395.
- (38) Wolf, M. O.; Fox, M. A. *J. Am. Chem. Soc.* **1995**, *117*, 1845.
- (39) Cooper, E.; Wiggs, R. A.; Hutt, D. A.; Parker, L.; Leggett, G. J.; Parker, T. L. *J. Mater. Chem.* **1997**, *7*, 435.
- (40) Cooper, E.; Leggett, G. J. *Langmuir* **1999**, *15*, 1024.
- (41) Hu, J.; Liu, Y.; Khemtong, C.; El Khoury, J. M.; McAfoos, T. J.; Taschner, I. S. *Langmuir* **2004**, *20*, 4933.
- (42) Sun, S.; Chong, K. S. L.; Leggett, G. J. *J. Am. Chem. Soc.* **2002**, *124*, 2414.
- (43) Sun, S.; Leggett, G. J. *Nano Lett.* **2002**, *2*, 1223.
- (44) Sun, S.; Leggett, G. J. *Nano Lett.* **2004**, *4*, 1381.
- (45) Huang, J.; Hemminger, J. C. *J. Am. Chem. Soc.* **1993**, *115*, 3342.
- (46) Lewis, M.; Tarlov, M. J.; Carron, K. J. *Am. Chem. Soc.* **1995**, *117*, 9574.
- (47) Hutt, D. A.; Leggett, G. J. *J. Phys. Chem.* **1996**, *100*, 6657.
- (48) Hutt, D. A.; Cooper, E.; Leggett, G. J. *J. Phys. Chem. B* **1998**, *102*, 174.
- (49) Cooper, E.; Leggett, G. J. *Langmuir* **1998**, *14*, 4795.
- (50) Zhang, Y.; Terrill, R. H.; Tanzer, T. A.; Bohn, P. W. *J. Am. Chem. Soc.* **1998**, *120*, 2654.
- (51) Norrod, K. L.; Rowlen, K. L. *J. Am. Chem. Soc.* **1998**, *120*, 2656.
- (52) Ferris, M. M.; Rowlen, K. L. *Appl. Spectrosc.* **2000**, *54*, 664.
- (53) Zhang, Y.; Terrill, R. H.; Bohn, P. W. *Chem. Mater.* **1999**, *11*, 2191.
- (54) Brewer, N. J.; Rawsterne, R. E.; Kothari, S.; Leggett, G. J. *J. Am. Chem. Soc.* **2001**, *123*, 4089.
- (55) Zharnikov, M.; Grunze, M. *J. Vac. Sci. Technol.* **2002**, *B20*, 1793.
- (56) Heister, K.; Rong, H.-T.; Buck, M.; Zharnikov, M.; Grunze, M.; Johansson, L. S. O. *J. Phys. Chem. B* **2001**, *105*, 6888.
- (57) Heister, K.; Zharnikov, M.; Grunze, M.; Johansson, L. S. O. *J. Phys. Chem. B* **2001**, *105*, 4058.
- (58) Frey, S.; Stadler, V.; Hesiter, K.; Eck, W.; Zharnikov, M.; Grunze, M.; Zeysing, B.; Terfort, A. *Langmuir* **2001**, *17*, 2408.
- (59) Frey, S.; Hesiter, K.; Zharnikov, M.; Grunze, M.; Tamada, K.; Colorado, R.; Graupe, M.; Shmakova, O. E.; Lee, T. R. *Isr. J. Chem.* **2000**, *40*, 81.
- (60) Zharnikov, M.; Frey, S.; Rong, H.; Yang, Y.-J.; Hesiter, K.; Buck, M.; Grunze, M. *Phys. Chem. Chem. Phys.* **2000**, *2*, 3359.
- (61) Horn, A. B.; Russell, D. A.; Shorthouse, L. J.; Simpson, T. R. E. *J. Chem. Soc., Faraday Trans.* **1996**, *92*, 4759.
- (62) Schoenfish, M. H.; Pemberton, J. E. *J. Am. Chem. Soc.* **1998**, *120*, 4502.
- (63) Poirier, G. E.; Herne, T. M.; Miller, C. C.; Tarlov, M. J. *J. Am. Chem. Soc.* **1999**, *121*, 9703.
- (64) Bordoli, R. S.; Vickerman, J. C. *Surf. Sci.* **1979**, *85*, 244.
- (65) Brown, A.; Vickerman, J. C. *Vacuum* **1981**, *31*, 429.
- (66) Shard, A. G.; Clarke, S.; Davies, M. C. *Surf. Interface Anal.* **2002**, *33*, 528.
- (67) Laibinis, P. E.; Whitesides, G. M.; Allara, D. L.; Tao, Y.-T.; Parikh, A. N.; Nuzzo, R. G. *J. Am. Chem. Soc.* **1991**, *113*, 7152.
- (68) Laibinis, P. E.; Fox, M.-A.; Folkers, J. P.; Whitesides, G. M. *Langmuir* **1991**, *7*, 3167.
- (69) Laibinis, P. E.; Bain, C. D.; Nuzzo, R. G.; Whitesides, G. M. *J. Phys. Chem.* **1995**, *99*, 7663.
- (70) Evans, S. D.; Ulman, A. *Chem. Phys. Lett.* **1990**, *170*, 462.
- (71) Alloway, D. M.; Hofmann, M.; Smith, D. L.; Gruhn, N. E.; Graham, A. L.; Colorado, R.; Wysocki, V. H.; Lee, T. R.; Lee, P. A.; Armstrong, N. R. *J. Phys. Chem. B* **2003**, *107*, 11690.
- (72) 5.1 eV: *CRC Handbook of Chemistry and Physics*, 77th ed.; CRC Press: Boca Raton, FL, 1996–97.
- (73) Zhou, X.-L.; Zhu, X.-Y.; White, J. M. *Surf. Sci. Rep.* **1991**, *13*, 73.
- (74) Kidd, R. T.; Lennon, D.; Meech, S. R. *J. Chem. Phys.* **2000**, *113*, 8276.